Strong Intramolecular Secondary Si···N Bonds in Trifluorosilylhydrazines

Krunoslav Vojinović,[a] Lorna J. McLachlan,[b] Sarah L. Hinchley,[b] David W. H. Rankin,[b] and Norbert W. Mitzel*[a]

Abstract: The simple silylhydrazines $F_3SiN(Me)NMe_2$ (**1**), $F_2Si(N(Me)NMe_2)_2$ (**2**), and $F_3SiN(SiMe_3)NMe_2$ (**3**) have been prepared by reaction of SiF_4 with $LiN(Me)NMe_2$ and $LiN(SiMe_3)NMe_2$, while $F_3SiN(SnMe_3)NMe_2$ (**4**) was prepared from SiF_4 and $(Me_3Sn)_2NNMe_2$ (**5**). The compounds were characterized by gas-phase IR and multinuclear NMR spectroscopy (^1H, ^{13}C, $^{14/15}N$, ^{19}F, ^{29}Si, ^{119}Sn), as well as by mass spectrometry. The crystal structures of compounds **1**–**5** were determined by X-ray crystallography. The structures of free molecules **1** and **3** were determined by gas-phase electron diffraction. The structures of **1**, **2**, and **4** were also determined by ab initio calculations at the MP2/6-311+G** level of theory. These structural studies constitute the first experimental proof for the presence of strong Si···N β-donor–acceptor bonds between the SiF_3 and geminal NMe_2 groups in silylhydrazines. The strength of these non-classical Si···N interactions is strongly dependent on the nature of the substituent at the α-nitrogen atom of the SiNN unit, and has the order **3** > **4** > **1**. The valence angles at these extremely deformed α-nitrogen atoms, and the Si···N distances are (crystal/gas): **1** 104.2(1)/106.5(4)°, 2.438(1)/2.510(6) Å; **3** 83.6(1)/84.9(4)°, 2.102(1)/2.135(9) Å; **4** 89.6(1)°, 2.204(2) Å.

Keywords: crystal structure · donor bonds · electron diffraction · hydrazines · silicon

Introduction

Silicon compounds that have atoms with donor functions in a geminal position to the silicon atom have a unique range of reactivity. This includes the α-fluoromethylsilanes, which form fluorosilanes upon expulsion of carbene,[1] as well as the nitrene generators that are based on silylhydroxylamines such as $R_3SiN(R)OSiR_3$,[2] and which lead to the formation of stable siloxanes. α-Aminocarbosilanes are particularly sensitive to hydrolysis of the Si–C bond.[3] This is an unusual type of reactivity as it is not normally observed when the geminal position to the silicon atom does not contain a donor group. A similar type of reactivity is used for the functionalization of polysilanes by *N,N*-dialkylhydroxylamine-catalysed alcoholysis of the Si–H bond.[4] Furthermore, a highly active type of cold-curing catalyst in silicone rubber polymerization is based on hydroxylaminosilanes.[5] Three-membered SiON ring transition states have been discussed and theoretically predicted[6] for the various types of silylhydroxylamine rearrangement reactions. One such transition state is a dyotopic one,[7] and leads to the formation of (alkoxy)aminosilanes.[8]

Despite the wide range of reactivity observed for these compounds, comparatively little is known about the special bonding situation that arises in silicon compounds that contain geminal donor centers. We could only prove the presence of strong non-classical Si···N interactions that lead to three-membered SiON rings in *O*-silylhydroxylamines that contain SiON units. The strongest β-donor bonds detected so far were found in $H_2Si(ONMe_2)_2$,[9] $ClH_2SiONMe_2$,[10] and $F_3SiONMe_2$.[11] $H_2Si(ONMe_2)_2$ was structurally characterized by X-ray crystallography and shows an average Si-O-N angle of 95.2°; this is much lower than what would be expected in the absence of any attractive Si···N interaction. In its crystal form, in which it is present as an *anti* conformer, $ClH_2SiONMe_2$ has a short Si···N distance of 2.028(1) Å and a valence angle at the oxygen atom of 79.7(1)°. In the same conformation, but as the free molecule (gas phase), the Si···N interaction is much weaker, and is characterized by an oxygen atom valence angle of 87.1(9)°. This interaction is found to be even weaker in the *gauche* conformer (Si-O-N

[a] Dr. K. Vojinović, Prof. Dr. N. W. Mitzel
Institut für Anorganische und Analytische Chemie
Westfälische Wilhelms-Universität Münster
Wilhelm-Klemm-Strasse 8, 48149 Münster (Germany)
Fax: (+49) 251-833-6007
E-mail: Mitzel@uni-muenster.de

[b] L. J. McLachlan, Dr. S. L. Hinchley, Prof. D. W. H. Rankin
School of Chemistry, University of Edinburgh
West Mains Road, Edinburgh EH9 3JJ (UK)
E-mail: d.w.h.rankin@ed.ac.uk.

Supporting information for this article is available on the WWW under http://www.chemeurj.org or from the author.

 DOI: 10.1002/chem.200400069

104.7(11)°). These findings indicate that the strength of the Si···N interaction is extremely dependent upon the electronic properties of the silicon substituent *anti* to the nitrogen center.

The strongest Si···N interaction in SiON systems found so far was in $F_3SiONMe_2$, in which the Si···N distance is 1.963(1) Å (Si-O-N 77.1(1)°).[11] Moreover, the strength of this interaction is extremely phase dependent, as was shown by subsequent structure determinations both in solution (Si-O-N 87.1°) and the gas phase (94.1(9)°). As a result, polarity and polarizability of the surrounding medium has significant influence on the molecules.[12]

In the search for Si···N attractive interactions in Si–N–N units, we investigated the simple systems $H_3SiMeNNMe_2$ and $(H_3Si)_2NNMe_2$. The three-dimensional structures of these compounds are determined by weak attractive interactions between the geminal silicon and nitrogen atoms.[13] However, as the SiH_3 groups are weak acceptors, much stronger interactions would be expected for compounds that bear more electron-withdrawing substituents at the silicon atoms. A clear picture could not be obtained in regards to the general presence of Si···N type β-donor interactions from earlier quantum-chemical calculations on silylhydrazines. On the basis that an Si-N-N angle of 115.1° was calculated at the QCISD/6-311+G** level of theory for the simplest system $H_3SiNHNH_2$, it was predicted that the attractive forces between silicon and the geminal nitrogen atoms would be negligible, but that these interactions would be stronger in SiNN compounds that bear an electronegative fluorine substituent on the silicon atom ($FH_2SiN(Me)NMe_2$; Si-N-N 103.1°). More intriguingly, when the hydrogen atom on the middle nitrogen atom of the SiNN unit in $FH_2SiN(SiH_3)NMe_2$ (MP2/6-311G**) was substituted by a silyl group, this angle was reduced to 93.9°. The reasons for this behavior remain unclear. Moreover, as the results of quantum-chemical calculations for β-donor systems were later shown to vary substantially with the level of theory and the size of the basis set applied, it seemed highly desirable to obtain sound experimental data to shed more light on the bonding that arises in SiNN systems.

Herein we demonstrate that such compounds contain strong secondary bonds that have the same characteristics as those present in hydroxylamines, but which are further dependent on the electronic properties of the substituents on the middle nitrogen atom of the SiNN unit.

Results and Discussion

Introduction of three fluoro substituents onto silicon atoms can make them extremely electrophilic. Reaction of silicon fluorides with lithiated hydrazines is known to lead to fluorinated silylhydrazines.[14] Thus, introduction of SiF_3 groups can be realized by using silicon tetrafluoride as a reagent. In this way we prepared trimethyl(trifluorosilyl)hydrazine [Eq. (1)].

$$F_4Si + LiNMeNMe_2 \rightarrow LiF + F_3SiNMeNMe_2 \quad (1)$$

A side reaction, in which silicon is doubly substituted, also occurs under these conditions [Eq. (2)], but the mixture of products can be separated by fractional condensation.

$$F_4Si + 2\,LiNMeNMe_2 \rightarrow 2\,LiF + F_2Si(NMeNMe_2)_2 \quad (2)$$

Lithiated *N,N*-dimethyl-*N′*-(trimethylsilyl)hydrazine was employed as a reagent to introduce an electropositive substituent onto the middle nitrogen atom of the SiNN unit. The resultant hydrazine contained two different silyl groups on one nitrogen atom [Eq. (3)].

$$F_4Si + LiN(SiMe_3)NMe_2 \rightarrow LiF + F_3SiN(SiMe_3)NMe_2 \quad (3)$$

We used a defluorostannylation reaction to introduce a trimethylstannyl group. In particular, we employed *N,N*-dimethyl-*N′*,*N′*-bis(trimethylstannyl)hydrazine (**5**) [Eq. (4)].

$$F_4Si + (Me_3Sn)_2NNMe_2\ (\mathbf{5}) \rightarrow Me_3SnF + F_3SiN(SnMe_3)NMe_2\ (\mathbf{4}) \quad (4)$$

At low temperatures (−78 °C), only one stannyl group is substituted in this reaction even in the presence of an excess of SiF_4. Some by-products were also detected in the spectra of the crude product, but these were not identified further. Compound **4** is unstable at ambient temperature and decomposes slowly to give less volatile products. All isolated compounds were identified by gas-phase IR and multinuclear NMR spectroscopy (^1H, ^{13}C, ^{15}N, ^{19}F, and ^{29}Si), as well as by mass spectrometry.

NMR spectra: As expected, the ^1H NMR spectra of **1**–**4** display only two signals. The fluorinated silicon groups give rise to a characteristic splitting of the ^{29}Si NMR resonances: a triplet ($^1J = 217.4$ Hz) for **2** at $\delta = -77.3$ ppm, and quartets for **1** ($\delta = -98.4$ ppm, $^1J = 193.8$ Hz), **3** ($\delta = -104.0$ ppm, $^1J = 200.4$ Hz), and **4** ($\delta = -98.1$ ppm, $^1J = 203.7$ Hz). The ^{29}Si NMR spectrum of **3** also contains a further resonance at $\delta = 7.32$ ppm for the Me_3Si group.

Coupling patterns due to the presence of fluorine atoms are also observed in the ^{15}N NMR spectra of these compounds. Compound **1** shows signals for each of the two nitrogen atoms of the hydrazine skeleton; one for the silicon-bound nitrogen atom at $\delta = -311.5$ ppm, and one for the NMe_2 group at $\delta = -326.4$ ppm. Both resonances are split into quartets by $^2J_{NSiF}$ (8.1 Hz) and $^3J_{NNSiF}$ (3.7 Hz) couplings. Although similar patterns are found for compounds **3** and **4**, in comparison to **1** the $^2J_{NSiF}$ coupling constant for compound **3** is much smaller (3.4 Hz) and the $^3J_{NNSiF}$ coupling constant is much larger (6.0 Hz), while for compound **4**, the coupling patterns could not be resolved.

The ^{15}N resonance chemical shifts for the silylated nitrogen atoms in **1**, **3**, and **4** are $\delta = -311.5$, −290.4, and −295.2 ppm, respectively. The variations reflect the diverse electronic environment imposed at this nitrogen atom by the different substituents [**1** (Me), **3** ($SiMe_3$), and **4** ($SnMe_3$)]. Unfortunately, as these values cannot be correlated purely to the different electronegativity of the bonded atoms (C, Si, and Sn, respectively), other factors must be

considered. The structural influence of these substituents on the coordination geometry of the nitrogen atoms will be discussed in the structural section below.

Only one resonance is observed in the ^{19}F NMR spectra of compounds **1**–**4**. This means that the fluorine atoms are all chemically equivalent on the NMR timescale at ambient temperature. This dynamic situation becomes important with respect to the interpretation of the solid-state structures described below.

Molecular and crystal structures: Single crystals of the compounds **1** (m.p. −52 °C), **2** (m.p. 19 °C), **3** (m.p. −10 °C), **4** (m.p. 2 °C), and **5** were grown in situ on the diffractometer in sealed Duran® capillaries. The crystal structures of these compounds were determined by X-ray crystallography. Compound **1** initially crystallized from the melt in the space group $P\bar{1}$, but during the data collection underwent a phase change over approximately 20 minutes, and gave rise to a marked change in the diffraction pattern. The space group of the new phase was *C*2/*c*. A good quality data set was obtained again when a second data collection was taken for the latter phase. The molecular structures for both phases of **1** are almost identical. Crystal structure diagrams of **1**, **2, 3, 4**, and **5** are shown in Figure 2, 1, 5, 8, and 9, respectively.

To compare the above structures with those of the free molecules, we determined the structures of **1** and **3** by gas-phase electron diffraction. In the course of these experiments, we also calculated the structures of **1** and **3** by various ab initio methods. The SARACEN method, which was recently described in a review,[15] was used to analyse the electron-diffraction data. Details for refinement of the electron-diffraction data and molecular model definitions are described in the Experimental Section as well as in the Supporting Information. The molecular geometries of the gas-phase structures of **1** and **3** are displayed in Figure 3 and 6, respectively. The radial distribution curves of the gas-phase electron diffraction refinements of **1** and **3** are shown in Figure 4 and 7, respectively.

*$F_2Si(N(Me)NMe_2)_2$ (**2**)*: As compound **2** is the only silane that contains two hydrazine groups, it will be discussed first. The crystal structure of **2** is shown in Figure 1 and some selected geometric parameters are listed in Table 1. Compound **2** is closely related to its chlorine analogue $Cl_2Si(N(Me)NMe_2)_2$,[16] but is not isomorphous. The Si–N bond lengths are short, but despite the presence of fluorine substituents, are slightly longer than those found in $Cl_2Si(N(Me)NMe_2)_2$. In contrast to the related hydroxylamine $H_2Si(ONMe_2)_2$, which has approximately C_S symmetry and a *Z* arrangement of the planar OSiON units, compound **2** adopts C_2 symmetry and can be described as a *gauche–gauche* conformer. In this respect it is similar to $Cl_2Si(N(Me)NMe_2)_2$. As indicated by the sum of angles at the nitrogen atoms directly attached to the silicon center (359.3°), these atoms have planar coordination environments, but they are far from being regular trigonal planar. For example, the three valence angles at the central nitrogen atom are 109.0(1) (Si-N-N), 130.9(1) (Si-N-C), and 119.4(1)° (C-N-N).

Table 1. Selected structural parameters for $F_2Si(N(Me)NMe_2)_2$ (**2**) as determined by low-temperature X-ray crystallography.

Distances [Å]		Angles [°]	
Si–F1	1.589(1)	Si-N1-N1	109.0(1)
Si–N1	1.679(1)	Si-N1-C1	130.9(1)
C1–N1	1.455(2)	C1-N1-N2	119.4(1)
N1–N2	1.432(1)	F1-Si-F1 a	105.4(1)
N2–C2	1.457(2)	C2-N2-C3	111.0(1)
N2–C3	1.460(2)	N1-N2-C2	112.2(1)
Si···N	2.540(1)	N1-N2-C3	112.1(1)

The differences between the Si-N-N angles in **2** (109.0(1)°) and $Cl_2Si(N(Me)NMe_2)_2$ (107.7(3) and 109.6(3)°) are almost negligible. This is surprising as substitution of the chlorine atoms in $Cl_2Si(NMeNMe_2)_2$ by fluorine would be expected to strengthen the interaction between the more positively charged silicon atom and the geminal nitrogen atoms. Systems in which attractive interactions are completely absent contain valence angles close to 120° around the nitrogen atoms. Thus, the Si···N distance of 2.540(1) Å in **2** arises as the result of only a very weak Si···N attractive interaction.

*$F_3SiN(Me)NMe_2$ (**1**)*: For the sake of simplicity in the discussion presented below, reference is only made to the *C*2/*c* phase (low-temperature phase) of the two crystal structures of **1**. In the solid state (Figure 2), compound **1** has an Si-N-N angle of 104.1(1)° and an Si···N distance of 2.436(1) Å, while in the gas phase (Figure 3), the Si-N-N angle is 106.5(4)° and the Si···N distance is 2.510(6) Å. This demonstrates that the geminal Si···N interaction is much weaker in $F_3SiN(Me)NMe_2$ (**1**) than in $F_3SiONMe_2$. Although large differences were frequently observed for the Si···N distances

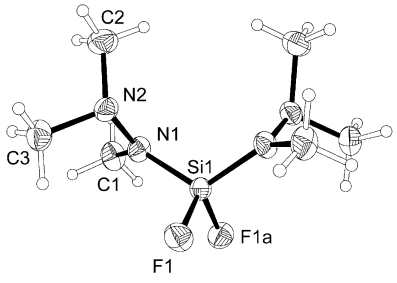

Figure 1. Crystal structure of **2**.

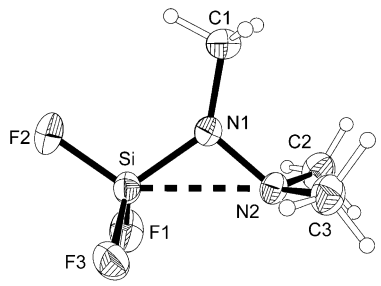

Figure 2. Crystal structure of **1** as determined by low-temperature X-ray diffraction.

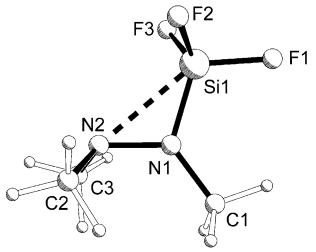

Figure 3. Gas-phase structure of **1** as determined by electron diffraction.

between the solid-state and gas-phase structures for SiON systems,[9–11] this was not the case for **1**.

The silyl group in both phases dictates that the α-nitrogen atom coordination is planar [sum of angles around nitrogen 359.5° (solid), 360.0° (gas)]. Although the weak Si···N interaction in **1** leads to a contraction of the Si-N-N angle that is comparatively small and comparable to that found in $H_3SiN(Me)NMe_2$ [Si-N-N 108.2(1)° (solid)], the α-nitrogen atom is quite deformed in both the gas and solid state. Whereas the Si-N-N angles discussed above are similar in the solid state (Figure 2), gas phase (Figure 3), and calculations (Figure 4), the Si-N-C and C-N-N angles around the α-nitrogen atom, although fairly consistent for the crystal structure and calculation (134.5(1) and 121.2(2)° (solid), respectively), differ markedly from the values determined in the gas phase (126.9(7) and 126.6(8)°, respectively). A further instance in which a substantial difference between the experimental and theoretical structures for a free molecule is observed will be described for compound **3** below.

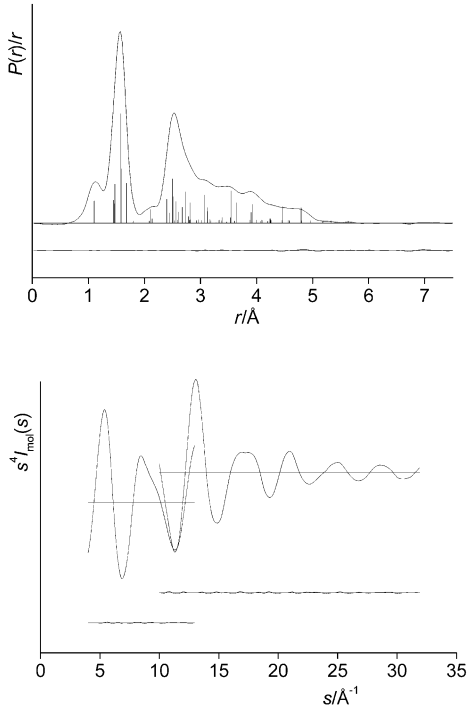

Figure 4. Radial distribution and molecular intensity curves for the gas-phase structure determination of **1**.

In contrast to the structural differences observed for the coordination geometry of the α-nitrogen atom, the coordination of the β-nitrogen atom is consistent in all phases and calculations (Table 2).

Table 2. Selected structural parameters for $F_3SiN(Me)NMe_2$ (**1**) as determined by low-temperature X-ray crystallography in two different phases, by ab initio calculations at the MP2/6-311+G** level of theory, and by gas-phase electron diffraction (GED). Distances are given in Å, angles in degrees.

Parameter	XRD $P\bar{1}$ phase	XRD *C2/c* phase	MP2 (r_e)	GED (r_a)
Si–F1	1.571(1)	1.568(1)	1.601	1.581(1)
Si–F2	1.566(2)	1.565(1)	1.598	1.578(1)
Si–F3	1.569(1)	1.565(1)		
Si–N1	1.644(1)	1.646(2)	1.681	1.677(3)
N1–N2	1.441(1)	1.439(2)	1.426	1.431(5)
N1–C1	1.456(2)	1.448(2)	1.456	1.467(2)
Si···N(1)	2.438(1)	2.436(1)	2.493	2.510(6)
Si-N1-N2	104.2(1)	104.1(1)	106.4	106.5(4)
C1-N1-N2	120.7(1)	121.2(2)	121.1	126.6(8)
Si-N1-C1	134.6(1)	134.5(1)	132.5	126.9(7)
N1-Si-F1	110.1(1)	109.9(1)	108.8	110.4(3)
N1-Si-F2	114.1(1)	115.7(1)	114.0	114.0(2)
N1-Si-F3	115.6(1)	113.8(1)		
C2-N2-C3	112.1(1)	111.9(1)	112.2	112.3(10)

*$F_3SiN(SiMe_3)NMe_2$ (**3**)*: In contrast to **2**, compound **3** contains a much stronger β-Si···N interaction. For example, in the solid state the Si-N-N angle is compressed to 83.6(1)°, and leads to a Si···N distance of only 2.102(1) Å (Figure 5);

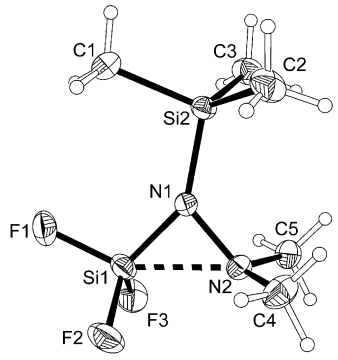

Figure 5. Crystal structure of **3** as determined by low-temperature X-ray diffraction.

these values are similar to those found for hydroxylamine $F_3SiONMe_2$. It should be noted, that in the latter compound the Si···N distance and Si-O-N angle are highly dependent upon the medium. That is, the Si···N interaction is much stronger in the solid state than in the gas phase. In contrast, the respective gas-phase values for **3** (84.9(4)° and 2.135(9) Å; Figure 6) are similar to those obtained for the solid state. However, experimental gas-phase values were found to differ significantly from ab initio calculations conducted at the MP2/6-311+G** level of theory (Figure 7). In particular, the Si-N-N angle was predicted to be 9° greater. Such large deviations between theoretical and experimental

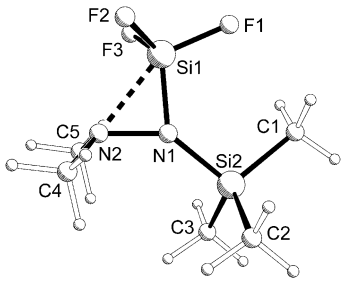

Figure 6. Gas-phase structure of **3** as determined by electron diffraction.

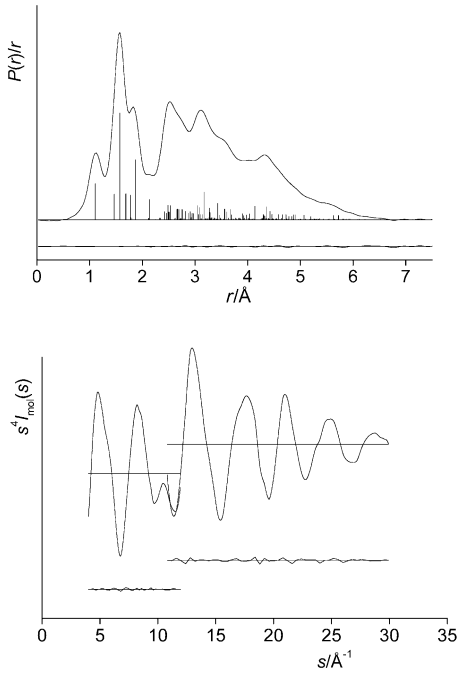

Figure 7. Radial distribution and molecular intensity curves for the gas-phase structure determination of **3**.

values for parameters directly connected to the non-classical geminal Si···N interactions have previously been observed, and can only be overcome at very high levels of theory.[11,17] Unfortunatley, at present these cannot feasibly be applied to molecules of the size of compound **3**.

Although normally observed for silylated nitrogen atoms, the distortion of the coordination sphere from the ideal trigonal planar in **3** is impressive, and is the result of an attractive Si···N interaction. Compression of the Si-N-N angle enclosed by the F_3Si and NMe_2 groups leads to a widening of the Si-N-Si angle enclosed by the Me_3Si and F_3Si groups (solid 145.9(1)°, gas 132.6(5)°), as well as a widening of the Si-N-N angle enclosed by the Me_3Si and NMe_2 groups (solid 130.0(1) °, gas 139.8(5)°). Therefore, a difference of more than 55° occurs between the two Si-N-N angles in this molecule in the gas phase. The implications of possible steric effects arising as a result of $SiMe_3$ substitution are discussed later in this paper.

As in compound **2**, the coordination sphere of the α-nitrogen atom is found to be planar in both the solid and gas phase, and the calculations confirm these observations. As outlined above, the (F_3)Si-N-N angle is similar in the solid and gas phase, but the other angles that define the coordination sphere of the α-nitrogen atom deviate drastically. The Si-N-Si angle in the solid state is extremely large (145.9(1)°), but in the gas phase is compressed by more than 13° (132.6(5)°) to be similar to the calculated gas-phase value (136.2°).

In contrast, the calculated gas-phase value for the (Me_3)Si-N-N angle (128.2°) is close to the solid-state value of 130.0(1)°, but is more than 11° smaller than the corresponding value in the gas-phase (139.8(5)°). Once again, the geometry of the NMe_2 group was found to be similar in all the methods of structure determination.

It is more appropriate to describe the geometry at the silicon atom as distorted trigonal bipyramidal than to describe it as a distorted tetrahedron with an additional Si···N contact. Two N-Si-F angles are close in value to 120° (118.2(1) and 117.2(1)°), therefore, these two fluorine atoms and the α-nitrogen atom make up the equatorial plane (the respective F-Si-F angle is 107.3(1)°). The fluorine atom with the lengthened Si–F bond is at an axial position (N-Si-F 108.3(1)°), while the β-nitrogen atom becomes the second axial ligand through a Si···N interaction. As a result, compound **3** has a much more pronounced distortion than **1**. Once again, this reflects the different strengths of the Si···N interactions between these molecules.

The geometry of the silicon atom reflects the hypercoordination. There are two different Si–F bond lengths in the solid state: two shorter ones (1.578 Å) to the fluorine atoms in a *gauche* orientation in the FSiNN unit, and a longer one (1.591(1) Å) to the *anti* fluorine atom. The longer bond length for the latter can be attributed to a *trans* effect as a result of the fifth ligand at silicon, namely the β-nitrogen atom. Although less pronounced, the differing Si–F bond lengths were also reflected in the calculations, but could not be resolved in the experimental gas-phase structure, in which all the Si–F distances were refined jointly to be one length.

The strong Si···N interaction observed also leads to a marked increase in the N–N bond length (1.487(2) Å in the solid state). This is substantially greater than the corresponding distance in **1** (1.438(2) Å) or **2** (1.432(1) Å), in which the Si···N interactions are weaker. Consequently, the Si–N bond in the SiNN ring is also lengthened (1.662(1) Å) in comparison to that observed in **1** (1.646(2) Å) (Table 3).

*$F_3SiN(SnMe_3)NMe_2$ (**4**)*: None of the intermolecular contacts in solid **1** and **3** are closer than the sum of the van der Waals radii, but molecules of **4** aggregate into endless chains through F···Sn interactions (Figure 8). This is intriguing, as the trifluorosilyl groups in all these compounds are better acceptors than the trimethylstannyl group in **4**. Although the structure-determining motif in compounds such as $F_3SiCH_2NMe_2$[18] that contain F_3Si–N linkages[19] has been to form dimers with Si–N contacts, the trimethylstannyl group in **4** makes contact with a terminal fluorine atom of the SiF_3

Table 3. Selected structural parameters for $F_3SiN(SiMe_3)NMe_2$ (**3**) as determined by low-temperature X-ray crystallography, by ab initio calculations at the MP2/6-311+G** level of theory, and by gas-phase electron diffraction (GED). Distances are given in Å, angles in degrees.

Parameter	XRD	MP2 (r_e)	GED (r_a)
Si–F1	1.591(1)	1.607	1.574(1)
Si–F2	1.578(1)	1.602	
Si–F3	1.577(1)	1.600	
Si2–C1	1.860(1)	1.869	1.873(1)
Si2–C2	1.855(1)	1.876	
Si2–C3	1.861(1)	1.876	
Si1–N	1.662(1)	1.690	1.690(6)
Si2–N	1.758(1)	1.779	1.769(6)
N1–N2	1.487(1)	1.462	1.463(3)
N2–C4	1.463(2)	1.459	1.463(3)
N2–C5	1.462(2)	1.461	
Si1···N2	2.102(1)	2.308	2.135(9)
Si1-N1-Si2	145.9(1)	136.2	132.6(5)
Si1-N1-N2	83.6(1)	93.9	84.9(4)
Si2-N1-N2	130.0(1)	128.2	139.8(5)
N1-Si1-F1	108.3(1)	109.7	109.0(5)
N1-Si1-F2	117.2(1)	114.9	113.9(5)
N1-Si1-F3	118.2(1)	114.2	116.0(6)
N1-Si2-C1	103.5(1)	105.8	104.4(6)
N1-Si2-C2	111.3(1)	110.5	107.4(8)
N1-Si2-C3	111.6(1)	110.9	109.1(9)
N1-N2-C4	112.5(1)	112.4	
N1-N2-C5	113.0(2)	112.8	

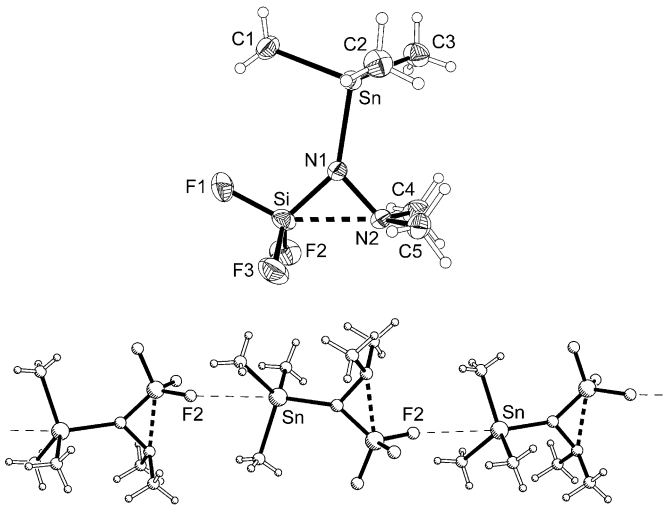

Figure 8. Crystal structure of **4** as determined by low-temperature X-ray diffraction, and aggregation of the molecules into chains by Sn···F intermolecular interactions.

unit in an adjacent molecule rather than with the more basic nitrogen atom of the NMe_2 group. The reason that these alternative donor–acceptor contacts are not used for the formation of intermolecular secondary bonding interactions demonstrates that in all three compounds the F_3Si and NMe_2 groups are already involved in a different type of interaction.

$F_3SiN(Me)NMe_2$ (**1**), $F_3SiN(SiMe_3)NMe_2$ (**3**), and $F_3SiN(SnMe_3)NMe_2$ (**4**) differ only in the group attached to the silicon-bound nitrogen atom, yet the Si-N-N angle of 89.6(1)° (solid state) in **4** is about 6° larger than in **3**, and more than 14° smaller than in compound **1**. Therefore, in regards to the strength of the intramolecular Si···N interaction, **4** adopts an intermediate position between **1** and **3**. This is also reflected in other parameters. For example, **4** has a relatively long N–N bond (1.472(3) Å) in comparison to that found in **1** (1.439(2) Å), but it is not as long as in compound **3** (1.487(1) Å). The same comparison is applicable to the Si–N bond, which is 1.651(2) Å in **4**, 1.662(1) Å in **3**, and 1.646(2) Å in **1**.

The coordination geometry at the silicon atom in **4** more closely resembles that of **3** than **1**. This is consistent with the observation that the N-Si-F angles (average of 117.0°) for the fluorine atoms in the gauche position are slightly smaller than those found in compound **3** (average of 117.6°), while the N-Si-F angle for the *anti* fluorine atom is slightly larger (109.6(1)° rather than 108.3(1)°), and that the difference between the *anti* and *gauche* Si–F bond lengths is smaller in compound **4** than in **3**. The very large Si-N-Sn (141.2(1)°) angle in **4** parallels the even larger Si-N-Si angle (145.9(1)°) in **3**, and the coordination geometry of the α-nitrogen atom is also planar.

The coordination geometry at the tin atom is distorted tetrahedral. Surprisingly, two of the N-Sn-C angles are as would be expected for a tetrahedron, while the angle in the approximate plane of molecular symmetry is slightly smaller (100.3(9)°). The reason for this distortion is not obvious, but could be the result of an attractive interaction between the fluorine atom F1 and one hydrogen atom of the respective methyl group (Table 4).

Table 4. Selected structural parameters for $F_3SiN(SnMe_3)NMe_2$ (**4**) as determined by low-temperature X-ray crystallography.

Distances [Å]		Angles [°]	
Si–F1	1.582(2)	Si-N1-Sn	141.2(1)
Si–F2	1.574(2)	N1-Si-F1	109.6(1)
Si–F3	1.577(2)	N1-Si-F2	116.9(1)
Sn–C1	2.123(3)	N1-Si-F3	117.2(1)
Sn–C2	2.132(3)	N1-Sn-C1	100.3(9)
Sn–C3	2.119(3)	N1-Sn-C2	107.8(1)
Si–N	1.651(2)	N1-Sn-C3	108.6(1)
Sn–N	2.078(2)	N1-N2-C4	111.3(2)
N1–N2	1.472(3)	N1-N2-C5	111.6(2)
N2–C4	1.457(3)		
N2–C5	1.455(3)		
Si···N2	2.204(3)		

Since the atom bonded to the α-nitrogen center of the SiNN unit is always a Group 14 element (**1**: C, **3**: Si, and **4**: Sn), the different strengths of the Si···N interaction in the F_3Si-N-NMe_2 skeleton should be related to electronic or steric properties of this binding atom or substituent. To obtain a reasonable estimate for the steric contribution, we calculated the molecular structure of $F_3SiN(SiH_3)NMe_2$ (**6**) at the MP2/6-311+G** level of theory and compared it with the structure determined for the silicon-methylated compound $F_3SiN(SiMe_3)NMe_2$ (**3**). Selected values can be found in Table 5. On the basis of these data, a purely steric argument can be excluded, as the parameters determined

Table 5. Comparison of selected calculated parameters for the molecular structures of $F_3SiN(SiMe_3)NMe_2$ (**3**) and $F_3SiN(SiH_3)NMe_2$ (**6**) at the MP2/6-311+G** level of theory. Distances are given in Å, angles in degrees.

Parameter	$F_3SiN(SiMe_3)NMe_2$ (**3**)	$F_3SiN(SiH_3)NMe_2$ (**6**)
$(F_3)Si-N$	1.690	1.693
$(Me_3/H_3)Si-N$	1.779	1.765
N–N	1.462	1.458
Si···N	2.308	2.397
$(F_3)Si-N-N$	93.8	98.8
$(Me_3/H_3)Si-N-N$	128.2	125.8
Si-N-Si	136.2	135.4
$N-Si-F_{in\ plane}$	109.7	109.7
N-N-C	111.8/112.4	111.7

were not significantly different. In particular, the $(F_3)Si-N-N$ angle was calculated to be 93.8° for **3** and 98.8° for **6**, while the Si···N distance was determined to be 2.308 and 2.397 Å for **3** and **6**, respectively. It should be noted that the extent by which the Si-N-N angles deviate from one another in the two compounds is only an approximation because attractive forces between silicon and nitrogen atoms, as well as angular potential, compensate for one another to some extent. However, if steric repulsion existed between the Me_3Si and H_3Si groups in **3** and **6** and the other groups in these molecules, the greatest deviation would be expected to be observed in this parameter. As a result, only a small steric effect with regard to the bulkier Me_3Si group in **3** could be deduced. Moreover, this conclusion neglects to take into account the different electronic properties of Me_3Si and H_3Si groups. The Si-N-Si angles should reflect the differences in repulsion between F_3Si and Me_3Si/H_3Si groups, but were found to be almost equal in **3** and **6** (136.2 and 135.4°, respectively). Similarly, the N-N-C angles would differ if a marked steric repulsion existed between the NMe_2 and Me_3Si/H_3Si groups, but they too were very similar (111.8/112.4° in **3** and 111.7° in **6**). In summary, the size of the substituent at the α-nitrogen atom has only a small steric effect. However, even in the absence of relevant steric contributions, calculations predict a marked Si···N attractive interaction in **3**.

*$(Me_3Sn)_2NNMe_2$ (**5**)*: In the course of our structure determination experiments, we were able to obtain crystals of compound **5** and determine its solid-state structure (Figure 9). This allowed us to compare $F_3SiN(SnMe_3)NMe_2$ (**4**) with $(Me_3Sn)N(SnMe_3)NMe_2$ (**5**), and thereby, to study the effects of exchanging the electrophilic F_3Si group for the less Lewis acidic Me_3Sn group, which has been shown to act as a weak acceptor in the geminal system $Me_3SnONMe_2$.[20]

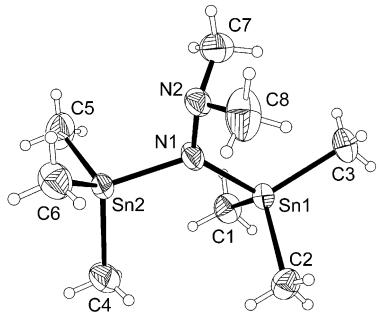

Figure 9. Crystal structure of **5**.

In compound **5**, the NMe_2 group leans slightly towards the Sn2 atom; this leads to one Sn-N-N angle being smaller and one larger (Sn2-N-N 109.5(4)°, Sn1-N-N 125.2(4)°). The $Sn1Me_3$ group has an almost tetrahedral coordination geometry around tin, with all the N-Sn-C angles lying between 107.7(3) and 108.1(3)°. However, as a result of steric repulsion between the NMe_2 and the $SnMe_3$ groups, the $Sn2Me_3$ group has a distorted coordination geometry around the tin atom with two small N-Sn-C angles (104.5(3) and 107.2(3)°) and one larger one (115.7(3)°). The conformation of the $Sn2Me_3$ group is different from that observed in compound **4**, as in **5** it is eclipsed with the N–N bond, whereas in **4** it is eclipsed with the N–Si bond. The result of this is that the Me_3Sn group distortion at the α-nitrogen atom is opposite to what is observed in compound **4**, namely the N-Sn-C angle is made wider rather than being compressed (Table 6).

Table 6. Selected structural parameters for $(Me_3Sn)_2NNMe_2$ (**5**) as determined by low-temperature X-ray crystallography.

Distances [Å]		Angles [°]	
Sn1–N1	2.048(6)	Sn1-N1-Sn2	125.2(4)
Sn2–N1	2.025(5)	Sn1-N1-N2	125.2(4)
N1–N2	1.428(7)	Sn2-N1-N2	109.5(4)
Sn1–C1	2.123(7)	N1-Sn1-C1	108.1(3)
Sn1–C2	2.134(7)	N1-Sn1-C2	107.8(3)
Sn1–C3	2.141(7)	N1-Sn1-C3	107.7(3)
Sn2–C4	2.129(7)	N1-Sn2-C4	104.5(3)
Sn2–C5	2.113(8)	N1-Sn2-C5	107.2(3)
Sn2–C6	2.120(7)	N1-Sn2-C6	115.7(3)
N2–C7	1.443(10)	N1-N2-C7	110.7(6)

Conclusion

Silylhydrazines are now the second class of silicon compounds, after silylhydroxylamines with SiON units, for which a relatively strong attractive interaction between silicon and a geminal donor center has been unequivocally proven by experiments. These findings will help the chemistry of this class of compounds to be better understood.

Silylhydrazines that contain electronegative substituents at silicon are compounds in which non-classical secondary bonds exist between silicon and the geminal nitrogen atoms. The strength of this interaction is dependent on the electronic properties and steric requirements of the substituent at the α-nitrogen atom, as well as on the nature of the silicon substituents. The nature of the binding atom seems to play the major role, whereas steric factors are not dominant for substituents up to the size of Me_3Si and Me_3Sn. The VSEPR model, which takes into consideration the polarity of the bond from the α-nitrogen atom towards its substituent, can be used to rationalize these results. In compound **1**, this bond polarity is much lower than in **3** and **4**, and thus, the maximum electron density in this bond is closer to the nitrogen atom in **3** and **4**. This subsequently results in the repulsion of the adjacent Si–N and N–N bonds, and together

with the attractive force between silicon and the β-nitrogen atoms, constitutes a further factor in shortening the Si···N distance.

It should be noted that a pronounced effect of this nature can probably only be observed in compounds in which no more than one nitrogen atom of the hydrazine skeleton has a silicon substituent attached. If both nitrogen atoms are silylated, then both will have an approximately planar coordination geometry, and thus, neither is able to act as a donor in an attractive Si···N interaction.

Further studies on geminal silicon donor systems will be directed towards aminomethylsilanes and oxymethylsilanes that contain Si–C–N and Si–C–O units, as these types of molecules are important building blocks in the synthesis of organosilicon compounds.

Experimental Section

All syntheses were carried out in a vacuum line that contained greaseless stopcocks (Young's taps) directly attached to the gas cell of an FTIR spectrometer (Midac Prospect FTIR). Tetrafluorosilane,[21] trimethylhydrazine,[22] *N*,*N*-dimethyl-*N*′-(trimethylsilyl)hydrazine,[23] *N*-lithio-*N*′,*N*′-dimethyl-*N*-(trimethylsilyl)hydrazine,[23] and *N*,*N*-dimethyl-*N*′,*N*′-bis(trimethylstannyl)hydrazine[24] were prepared as described in the respective literature procedures. Dimethyl ether gas was dried over CaH_2, condensed, and degassed prior to use. The other solvents were dried over CaH_2. All NMR spectra were recorded at 21 °C on a JEOL JNM-LA-400 spectrometer in sealed tubes with C_6D_6 being directly condensed onto the frozen samples from an Na/K alloy.

$F_3SiN(Me)NMe_2$ (1) and $F_2Si(N(Me)NMe_2)_2$ (2): *n*-Butyllithium (12.5 mL of a 1.6 M solution in *n*-hexane, 20 mmol) was added dropwise to a solution of trimethylhydrazine (1.5 g, 20 mmol) in *n*-hexane (20 mL) at −78 °C. The reaction mixture was then warmed to room temperature and stirred for 1 h, after which time all volatiles were removed under vacuum. Dimethyl ether (15 mL) and then a 1.5 molar excess of SiF_4 (3.1 g, 29 mmol) were condensed onto the freshly prepared $LiN(Me)NMe_2$ (1.5 g, 19 mmol, 96 %) at −196 °C. The reaction mixture was then warmed to −96 °C (toluene slush) and subsequently allowed to reach −30 °C over a period of several hours, at which temperature it was stirred for 1 h. All volatiles were then condensed and separated by fractional condensation (−10, −78, and −196 °C traps). The −10 °C cold trap retained the least volatile $F_2Si(N(Me)NMe_2)_2$ (**2**) (1.2 g, 5.7 mmol, 30 %) as a colorless, crystalline solid (m.p. 19 °C). ^{1}H NMR (C_6D_6): $\delta = 2.27$ (s, 6H; Me_2N), 2.42 ppm (t, $^4J_{HCNSiF} = 1.5$ Hz, 3H; MeN); ^{13}C NMR (C_6D_6): $\delta = 22.2$ (q, $^1J_{CH} = 134.9$ Hz, MeN), 43.1 ppm (qq, $^1J_{CH} = 133.4$ and $^3J_{CNCH} = 4.8$ Hz, Me_2N); ^{14}N NMR (C_6D_6): $\delta = -312.2$ ppm (s); ^{19}F NMR (C_6D_6): $\delta = -78.0$ ppm (s); ^{29}Si NMR (C_6D_6): $\delta = -77.3$ ppm (t, $^1J_{SiF} = 217.4$ Hz); IR (gas, selected data): $\tilde{\nu}$ = 2955m, 2874m, 2791w, 870s, 714w cm^{-1}; GCMS (70 eV): *m*/*z*: 212 $[M]^+$, 169 $[M-NMe_2]^+$, 154 $[M-(NMe_2-Me)]^+$, 138 $[M-NMeNMe_2]^+$.

The −78 °C cold trap contained $F_3SiN(Me)NMe_2$ (**1**) (0.52 g, 3.3 mmol, 15 %) as a colorless liquid that was very sensitive to air and moisture (m.p. −52 °C). ^{1}H NMR (C_6D_6): $\delta = 2.05$ (s, 6H; Me_2N), 2.09 ppm (q, $^4J_{HCNSiF} = 1.6$ Hz, 3H; MeN); ^{13}C NMR (C_6D_6): $\delta = 21.1$ (q, $^1J_{CH} = 135.7$ Hz, MeN), 42.4 ppm (qq, $^1J_{CH} = 134.5$ and $^3J_{CNCH} = 4.4$ Hz, Me_2N); ^{15}N{^{1}H} NMR (DEPT, C_6D_6): $\delta = -311.5$ (q, $^2J_{NSiF} = 8.1$ Hz), −326.4 ppm (q, $^3J_{NNSiF} = 3.7$ Hz); ^{19}F NMR (C_6D_6): $\delta = -83.4$ ppm (s); ^{29}Si NMR (C_6D_6): $\delta = -98.4$ ppm (q, $^1J_{SiF} = 193.8$ Hz); IR (gas, selected data): $\tilde{\nu}$ = 2970m, 2861m, 2791w, 971ss, 890s, 715w cm^{-1}.

$F_3SiN(SiMe_3)NMe_2$ (3): A twofold excess of SiF_4 (7.1 g, 66 mmol) was condensed onto a frozen (−196 °C) solution of freshly prepared $LiN(SiMe_3)NMe_2$ (4.6 g, 33 mmol) in Me_2O (15 mL). The mixture was warmed to −96 °C, and was then allowed to warm to −30 °C over a period of 5 h, at which temperature it was stirred for a further 1 h. All volatiles were condensed and separated by fractional condensation (−50, −96, and −196 °C traps). Compound (**3**) (2.1 g, 10 mmol, 30 %) was isolated in the −50 °C trap as a colorless, very smelly liquid (m.p. −10 °C). ^{1}H NMR (C_6D_6): $\delta = 0.06$ (s, 9H; Me_3Si), 2.30 ppm (s, 6H; Me_2N); ^{13}C NMR (C_6D_6): $\delta = 1.19$ (q, $^1J_{CH} = 118.7$ Hz, Me_2N), 48.2 ppm (q, $^1J_{CH} = 135.6$ Hz, MeN); ^{15}N{^{1}H} NMR (DEPT, C_6D_6): $\delta = -290.4$ (q, $^2J_{NSiF} = 3.4$ Hz, NSi_2), −319.6 ppm (q, $^3J_{NSiF} = 6.0$ Hz, NC_2); ^{19}F NMR (C_6D_6): $\delta = -76.8$ ppm (s); ^{29}Si NMR (C_6D_6): $\delta = -7.32$ (s, $SiMe_3$), −104.0 ppm (q, $^1J_{SiF} = 200.4$ Hz); IR (gas, selected data): $\tilde{\nu}$ = 2963m, 2874m, 2789w, 2795w, 1789w, 1259w, 964m, 758w cm^{-1}; GCMS (70 eV, selected data): *m*/*z*: 216 $[M]^+$, 201 $[M-Me]^+$, 73 $[Me_3Si]^+$.

$F_3SiN(SnMe_3)NMe_2$ (4): A slight excess of SiF_4 (0.52 g, 5 mmol) was condensed onto a solution of $(Me_3Sn)NNMe_2$ (1.68 g, 4.35 mmol) in Et_2O (15 mL) at −196 °C. The reaction mixture was warmed to −78 °C, then over a period of several hours it was warmed to room temperature and stirred overnight. After the mixture was cooled to −55 °C, the solvent was removed under reduced pressure. The residue was then condensed into another flask, pentane (5 mL) was added, and the mixture was stored at −78 °C for two days, after which time large colorless crystals were obtained. These melted at 2 °C to give a very air- and moisture-sensitive liquid (0.28 g, 0.9 mmol, yield 21 %) that slowly decomposed at room temperature. ^{1}H NMR (C_6D_6): $\delta = 0.17$ (s, Me_3Si), 2.29 ppm (s, NMe_2); ^{15}N{^{1}H} NMR (DEPT, C_6D_6): $\delta = -295.2$ (br s), −318.5 ppm (br s); ^{19}F NMR (C_6D_6): $\delta = -79.35$ ppm (s); ^{29}Si NMR (C_6D_6): $\delta = -98.11$ ppm (q, $^1J_{SiF} = 203.7$ Hz); ^{119}Sn NMR (C_6D_6): $\delta = 67.44$ ppm (s); GCMS (70 eV): *m*/*z*: 308 $[M]^+$, 293 $[M-Me]^+$, 220 $[M-F_3Si]^+$, 165 $[Me_3Sn]^+$.

Crystal structures: Single crystals were generated by slowly cooling the melt after a solid–liquid equilibrium of the sample in a sealed Duran® capillary was established. All but one of the crystals (an optically selected very small seed crystal) were then melted by locally warming the sample. The data collection was undertaken with a DIP 2020 diffractometer (Enraf Nonius) with an image-plate detector. Graphite-monochromated $Mo_{K\alpha}$ radiation was used ($\lambda = 0.71073$ Å). Intensity corrections were applied by means of the SCALEPACK program.[25] The structures were solved by direct methods and refined using the full-matrix least-squares procedure (SHELXTL[26]) against F^2. Plots of the molecular structures are represented by thermal ellipsoids at the 50 % probability level. Details for the crystal data and refinements are provided in Table 7.

CCDC-229353 (**1**), CCDC-229354 (**1**), CCDC-229352 (**2**), CCDC-229355 (**3**), CCDC-229357 (**4**), and CCDC-229356 (**5**) contain the supplementary crystallographic data for this paper. These data can be obtained free of charge via www.ccdc.can.ac.uk/conts/retrieving.html (or from the Cambridge Crystallographic Center, 12 Union Road, Cambridge CB21EZ, UK; Fax: (+44) 1223-336033; or deposit@ccdc.cam.ac.uk).

Gas-phase electron diffraction experiment: The Edinburgh gas-diffraction apparatus[27] was used to collect data for **1** and **3**. The sample and nozzle temperatures were held at 239 and 293 K, respectively, for **1**, and 273 and 293 K, respectively, for **3**. An accelerating voltage of about 40 kV (electron wavelength ca. 6.0 pm) was used and the scattering intensities for both compounds were recorded at nozzle-to-film distances of 128.2 and 285.2 mm for **1** and 127.7 and 285.4 mm for **3** on Kodak Electron Image film. Three films were collected at each nozzle-to-plate distance. The weighting points for the off-diagonal weight matrices, correlation parameters, and scale factors for the two camera distances for both compounds are given in Table 8. For calibration purposes and in order to minimise any systematic errors in wavelength and camera distances, the scattering patterns of benzene were also collected and analysed in the same way. The electron-scattering patterns were converted into digital form at the Institute of Astronomy, Cambridge, UK using a PDS densitometer and a scanning program described elsewhere.[28] Data reduction and least-squares refinements were carried out using standard programs.[29] The scattering factors of Ross et al. were employed.[30]

Acknowledgements

We are grateful for support from the Deutsche Forschungsgemeinschaft and Fonds der Chemischen Industrie, as well as the U.K. Engineering and Physical Sciences Research Council. We would also like to thank The Royal Society of Chemistry for a Journal Grant (N.W.M.), which enabled us to meet, exchange samples, and discuss the gas-phase structures.

Table 7. Crystal and refinement data for the solid-state structures of compounds **1**–**5**.

Compound	$F_3SiN(Me)NMe_2$ (**1**)	$F_3SiN(Me)NMe_2$ (**1**)	$F_2Si(N(Me)NMe_2)_2$ (**2**)	$F_3SiN(SiMe_3)NMe_2$ (**3**)	$F_3SiN(SnMe_3)NMe_2$ (**4**)	$(Me_3Sn)_2NNMe_2$ (**5**)
formula	$C_3H_9F_3N_2Si$	$C_3H_9F_3N_2Si$	$C_6H_{18}F_2N_4Si$	$C_5H_{15}F_3N_2Si_2$	$C_5H_{15}F_3N_2SiSn$	$C_8H_{24}N_2Sn_2$
formula weight	158.21	158.21	212.32	216.37	306.97	385.67
crystal system	triclinic	monoclinic	monoclinic	orthorhombic	orthorhombic	monoclinic
space group	$P\bar{1}$	$C2/c$	$C2/c$	$Pbca$	$Pbca$	$P2_1/c$
a [Å]	6.3676(3)	19.5157(13)	9.0946(2)	13.2781(1)	13.5469(2)	15.6424(7)
b [Å]	6.5163(4)	6.5080(5)	11.2124(3)	10.9471(1)	11.1830(1)	7.5735(2)
c [Å]	10.2513(5)	11.4913(9)	11.6720(2)	14.7906(2)	14.7578(2)	12.7078(4)
α [°]	79.091(3)	90	90	90	90	90
β [°]	72.896(3)	94.907(3)	111.8907(12)	90	90	105.9583(13)
γ [°]	63.708(5)	90	90	90	90	90
V [Å^3]	363.63(3)	1454.14(19)	1104.40(4)	2149.91(4)	2235.73(5)	1447.55(9)
ρ_{calcd} [g cm^{-3}]	1.445	1.445	1.277	1.337	1.824	1.770
Z	2	8	4	8	8	4
μ [mm^{-1}]	0.299	0.299	0.207	0.328	2.390	3.417
temperature [K]	143(2)	143(2)	153(2)	143(2)	143(2)	143(2)
θ range [°]	4.17–31.51	3.30–30.56	3.02–31.65	2.75–31.58	2.74–31.91	3.01–28.48
measured reflect.	4093	57476	23749	91945	84634	62034
unique reflect.	1798	2163	1710	3291	3816	3541
observed reflect.	1658	1946	1595	3086	3694	3218
R_{int}	0.021	0.040	0.031	0.039	0.052	0.104
parameters	118	119	96	170	135	126
$R\,[I>2\sigma(I)]/wR2$	0.039/0.104	0.051/0.135	0.035/0.098	0.037/0.101	0.030/0.065	0.051/0.117
ρ_{fin} (max/min) [eÅ^{-3}]	+0.21/−0.31	+0.50/−0.37	+0.33/−0.34	+0.33/−0.42	+0.93/−0.58	+0.84/−0.85
CCDC-No.	229353	229354	229352	229355	229357	229356

Table 8. GED experimental conditions for **1** and **3** (Δs denotes the spacing of the data points in s, s_{min}, and s_{max} to give the minimum and maximum of the s range in which the data were recorded).

Compound	**1**		**3**	
camera distance [mm^{-1}]	128.18	285.15	127.66	285.38
Δs [nm^{-1}]	4	2	4	2
s_{min} [nm^{-1}]	100	40	108	40
s_1 [nm^{-1}]	120	60	128	60
s_2 [nm^{-1}]	272	110	256	102
s_{max} [nm^{-1}]	320	130	300	120
correlation paramater	−0.2800	0.2707	−0.2322	0.1397
scale factor	0.696(5)	0.754(1)	0.714(19)	0.868(8)
electron wavelength [pm^{-1}]	6.016	6.016	6.016	6.016
R_G	0.015		0.021	
R_D	0.013		0.023	

[1] a) R. N. Haszeldine, J. C. Young, *J. Chem. Soc.* **1959**, 394; b) H. Beckers, H. Bürger, *J. Organomet. Chem.* **1990**, *385*, 207.

[2] Y. H. Chang, F.-T. Chiu, G. Zon, *J. Org. Chem.* **1981**, *46*, 352.

[3] N. F. Lazareva, V. P. Baryshok, M. G. Voronkov, *Russ. Chem. Bull.* **1995**, *104*, 374.

[4] Y. Hamada, S. Mori, *Proceedings of the 29th Organosilicon Symposium*, March **1996**, *Evanston*, *USA*.

[5] A collection of patent literature references can be found in: M. G. Voronkov, E. A. Maletina, V. K. Roman, *Heterosiloxanes, Vol. 2: Derivates of Nitrogen and Phosphorus*, Harwood, Chur, Switzerland **1991.**

[6] S. Schmatz, C. Ebker, T. Labahn, H. Stoll, U. Klingebiel, *Organometallics* **2003**, *22*, 490.

[7] a) R. West, P. Novakovski, *J. Am. Chem. Soc.* **1976**, *98*, 5616; b) R. West, P. Novakovski, P. Boudjouk, *J. Am. Chem. Soc.* **1976**, *98*, 5620; c) R. West, P. Boudjouk, *Intra-Sci. Chem. Rep.*, **1973**, 765.

[8] a) S. Schmatz, F. Diedrich, C. Ebker, U. Klingebiel, *Eur. J. Inorg. Chem.* **2002**, 876; b) R. Wolfgramm, T. Müller, U. Klingebiel, *Organometallics*, **1998**, *17*, 3222.

[9] N. W. Mitzel, U. Losehand, *Angew. Chem.* **1997**, *109*, 2897; *Angew. Chem. Int. Ed. Engl.* **1997**, *36*, 2807.

[10] N. W. Mitzel, U. Losehand, *J. Am. Chem. Soc.* **1998**, *120*, 7320.

[11] N. W. Mitzel, U. Losehand, A. Wu, D. Cremer, D. W. H. Rankin, *J. Am. Chem. Soc.* **2000**, *122*, 4471.

[12] K. R. Leopold, M. Canagaratna, J. A. Phillips, *Acc. Chem. Res.* **1997**, *30*, 57.

[13] N. W. Mitzel, *Chem. Eur. J.* **1998**, *4*, 692.

[14] a) E. Gellermann, U. Klingebiel, H. Noltemeyer, S. Schmatz, *J. Am. Chem. Soc.* **2001**, *123*, 382; b) U. Klingebiel, H. Hluchy, A. Meller, *Chem. Ber.* **1978**, *111*, 906; c) E. Gellermann, U. Klingebiel, T. Pape, F. D. Antonia, T. Schneider, S. Schmatz, *Z. Anorg. Allg. Chem.* **2001**, *627*, 2581; d) H. Witte-Abel, U. Klingebiel, M. Schaefer, *Z. Anorg. Allg. Chem.* **1998**, *624*, 271; e) K. Bode, U. Klingebiel, H. Witte-Abel, M. Sluth, M. Noltemeyer, R. Herbst-Irmer, M. Schäfer, W. Shomaky, *Phosphorus Sulfur Silicon Relat. Elem.* **1996**, *108*, 121; f) K. Kipping, C. Drost, U. Klingebiel, M. Noltemeyer, *Z. Anorg. Allg. Chem.* **1996**, *622*, 1215.

[15] N. W. Mitzel, D. W. H. Rankin, *J. Chem. Soc. Dalton Trans.* **2003**, 3650.

[16] N. W. Mitzel, B. A. Smart, A. J. Blake, S. Parsons, D. W. H. Rankin, *J. Chem. Soc. Dalton Trans.* **1996**, 2095.

[17] M. Korth, S. Grimme, K. Vojinović, N. W. Mitzel, unpublished results.

[18] W. S. Sheldrick, W. Wolfsberger, *Z. Naturforsch. B* **1977**, *32*, 22.

[19] K. Vojinović, N. W. Mitzel, D. W. H. Rankin, unpublished results.

[20] N. W. Mitzel, U. Losehand, A. Richardson, *Organometallics* **1999**, *18*, 2610.

[21] U. Losehand, Thesis, Technische Universität München, **1999**.

[22] a) R. T. Beltrami, E. R. Bissell, *J. Am. Chem. Soc.* **1956**, *78*, 2467; b) J. B. Claas, J. G. Aston, T. S. Oakwood, *J. Am. Chem. Soc.* **1953**, *75*, 2937.

[23] U. Wannagat, F. Höfler, *Monatsh. Chem.* **1966**, *97*, 976.

[24] N. Wiberg, M. Veith, *Chem. Ber.* **1971**, *104*, 3191.

[25] SCALEPACK: Z. Otwinowski, W. Minor, *Methods Enzymol.* **1997**, *276*, 307.
[26] SHELXTL-PC 4.1 Siemens Analytical X-Ray Instruments Inc. **1990**.
[27] C. M. Huntley, G. S. Laurenson, D. W. H. Rankin, *J. Chem. Soc. Dalton Trans.* **1980**, 945.
[28] J. R. Lewis, P. T. Brain, D. W. H. Rankin, *Spectrum* **1997**, *15*, 7.
[29] A. S. F. Boyd, G. Laurenson, D. W. H. Rankin, *J. Mol. Struct.* **1981**, *71*, 217.
[30] A. W. Ross, M. Fink, R. Hilderbrandt, *International Tables for X-Ray Crystallography, Vol. C*, (Ed.: A. J. C. Wilson), Kluwer, Dodrecht, Boston, **1992**, p. 245.

Received: January 20, 2004
Published online: April 29, 2004

